DELPHI Collaboration

DELPHI 2001-000
January 28, 2002

DRAFT #3

Inclusive J/ψ Production in Two-Photon Collisions at LEP

M. Chapkin, S.-U. Chung, P. Gavillet,
V. Obraztsov, D. Ryabchikov, A. Sokolov, S. Todorovova

Abstract

Inclusive J/ψ production in photon-photon collisions has been observed by the DELPHI collaboration at LEP II beam energies. A clean signal from the reaction $\gamma\gamma \to J/\psi + X$ is seen. The number of observed events $N(J/\psi \to \mu^+\mu^-)$ is 36 ± 7 for the integrated luminosity of 617 pb^{-1}, yielding a cross section of $\sigma(J/\psi + X) = 45.3 \pm 18.4$ pb. Based on a study of the event shapes of different types of $\gamma\gamma$ processes in the PYTHIA program, we conclude that $(74 \pm 22)\%$ of the observed J/ψ events are due to the 'resolved' photons, the dominant contribution of which is evidently a single color-octet gluon within the photon.

Submitted to Summer Conferences of 2001

1 Introduction

An important component of the e^+e^- collisions at LEP II energies is the two-photon fusion process. It has been pointed out that two-photon production of inclusive J/ψ's

$$e^+ + e^- \to e^+ + e^- + \gamma_1 + \gamma_2 \tag{1}$$

followed by

$$\gamma_1 + \gamma_2 \to J/\psi + X \tag{2}$$

is a sensitive channel for investigating the gluon distribution in the photon [1].

There are two important processes leading to inclusive J/ψ production. The corresponding typical diagrams are given in Figs. 1 and 2. Less important diagrams are not considered here. Our motivation is to illustrate two major categories of diagrams which are used to fit the observed $p_T^2(J/\psi)$ distribution in our data. The first process is undoubtedly attributable to the vector-meson dominance (VMD) model [2]

$$\gamma_1 \to c + \bar{c}, \qquad \gamma_2 \to q + \bar{q} \qquad \text{and} \qquad \gamma_1 + \gamma_2 \to J/\psi + q + \bar{q} \tag{3}$$

as shown in Fig. 1. The vertices for γ_1 and γ_2 are connected by Pomeron exchange or diffractive dissociation of photons. The final-state parton pairs $c+\bar{c}$ and $q+\bar{q}$ are both in the state of $J^{PC} = 1^{--}$, which means that the latter is dominated by the low-mass vector mesons ρ^0, ω and ϕ but a more general inclusive hadronization of the partons may also be important.

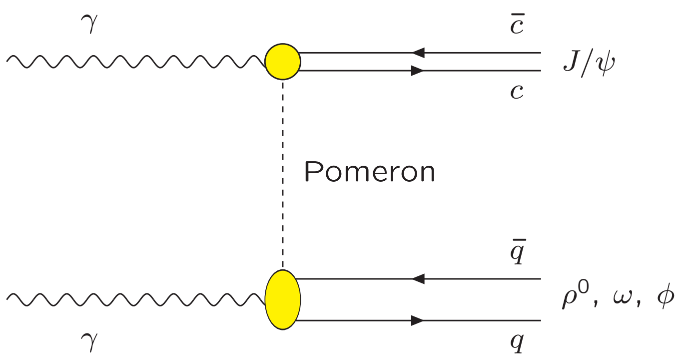

Figure 1: Inclusive J/ψ production in $\gamma\gamma$ processes through vector-meson dominance.

The second process is due to the color-octet model [3]. It proceeds through the so-called 'resolved' contribution of the photons, in which the intermediate photons are 'resolved' into their constituent partons.

$$\gamma_1 + g_\gamma \to c + \bar{c}, \qquad \gamma_2 + g_\gamma \to q + \bar{q}, \qquad \text{and} \qquad \gamma_1 + \gamma_2 \to J/\psi + q + \bar{q} \tag{4}$$

as shown in Fig. 2. It is seen that this process requires production of a 'resolved' gluon

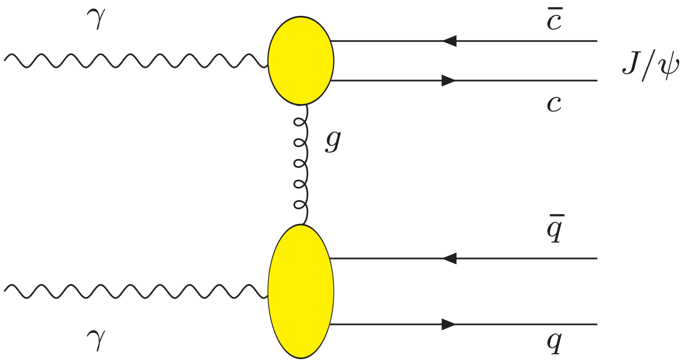

Figure 2: Inclusive J/ψ production in $\gamma\gamma$ processes via gluon content of the photon, i.e. 'resolved' contributions. Presence of additional soft gluon(s) is required for color neutralization.

(g_γ) from both photons. Thus, this production mechanism provides a sensitive probe of the gluon content of the photon.

The purpose of this letter is to report observation of inclusive J/ψ production from the two-photon fusion process; to give its production characteristics along with the cross section; and finally to assess the relative importance of the production processes discussed above.

2 Experimental Procedure

The analysis presented here is based on the data taken with the DELPHI detector [4, 5] during the years 1996–2000 for which $\sqrt{s}$ for LEP ranged from 161 to 207 GeV, excluding the part of the data collected in the last period of 2000 when one of the TPC sectors was not in operation. The total integrated luminosity used in the analysis is 617 pb^{-1}.

The charged particle tracks were measured in the 1.2–T magnetic field by a set of tracking detectors including the TPC and the forward/backward chambers FCA and FCB. The following criteria were applied:

(a) particle momentum $p > 200$ MeV/c;
(b) relative error of a track momentum $\Delta p/p < 100\%$;
(c) impact parameter of a track, transverse to the beam axis $\Delta_{xy} < 3$ cm;
(d) impact parameter of a track, along the beam axis $\Delta_z < 7$ cm;
(e) polar angle of a track, with respect to the beam axis $10^\circ < \theta < 170^\circ$;
(f) track length $\ell > 30$ cm.

The neutral particles (γ, π^0, K^0_L, n) were selected by demanding that the calorimetric information, not associated with charged particle tracks, satisfy the following cuts:

(g) E(neutral) > 0.2 GeV for the electromagnetic showers unambiguously identified as photons;
(h) E(neutral) > 0.5 GeV for all the other showers;
(i) polar angle of a neutral track, with respect to the beam axis $10^\circ < \theta < 170^\circ$.

In order to ensure a very high trigger efficiency, the selected events were required to satisfy at least *one* of a set of the four following criteria:

(j_1) one or more charged tracks in the barrel region ($40° < \theta < 140°$) with $p_t > 1.2$ GeV/c, is found;

(j_2) one or more neutral tracks in the the Forward Electromagnetic Calorimeter (FEMC) ($10° < \theta < 36°$ and $144° < \theta < 170°$) with energy greater than 10 GeV, is found;

(j_3) the sum of the number of charged tracks in barrel with $p_t > 1$ GeV/c and charged tracks in forward region ($10° < \theta < 40°$ or $140° < \theta < 170°$) with $p_t > 2$ GeV/c and neutrals in the forward electromagnetic calorimeter (FEMC) with $E > 7$ GeV is greater than one;

(j_4) the sum of the number of charged tracks in barrel with $p_t > 0.5$ GeV/c and charged tracks in forward with $p_t > 1$ GeV/c and neutral tracks in FEMC with $E > 5$ GeV is greater than four.

The trigger efficiency for the events which passed the above requirements is bigger than 98%.

The hadronic two-photon events are characterized by low track multiplicity and low visible invariant mass. Consequently, the following additional cuts were applied:

(k) the visible invariant mass, W_{vis}, calculated from the four-momentum vectors of the measured charged and neutral tracks, is less than 35 GeV/c^2;

(l) the number of charged tracks N satisfies $4 \leq N_{\text{ch}} \leq 30$;

(m) the sum of the transverse energy components with respect to the beam direction for all charged particles ($\sum E_T^{\text{vis}}$) is greater than 3 GeV.

The comparison of the W_{vis} distributions—after the cuts $N_{\text{ch}} \geq 4$ and $\sum E_T^{\text{vis}} > 3$ GeV—both for the data and the events simulated by PYTHIA (Fig. 3) shows that the cut $W_{\text{vis}} \leq 35$ GeV/c^2 rejects major part of the non-two-photon events.

A total of 274 510 events remain in the data sample after applying all these cuts. The main background comes from the process $e^+e^- \to Z^0\gamma$ and amounts to ∼1.2% of the selected $\gamma\gamma$ events. The backgrounds from the $e^+e^- \to W^+W^-$ and other processes are negligible, as seen in Fig. 3.

J/ψ candidates have been selected using the $\mu^+\mu^-$ decay channel. For the muon selection the following criteria were imposed:

(n) the track should satisfy the standard DELPHI muon-tagging algorithm [5] or be identified as a muon by the hadronic calorimeter [6];

(o) the track should not come from any reconstructed secondary vertex or be identified as a kaon, proton or electron by standard DELPHI identification packages;

(p) at least two charged particles with zero net charge should be identified as muons.

3 Inclusive J/ψ Production

We give in Fig. 4 the invariant mass distribution for $\mu^+\mu^-$ from the DELPHI data selected as outlined in the previous section. It is seen that the J/ψ is produced over little background. A fit to the $M(\mu^+\mu^-)$ distribution with a Gaussian for the signal and a polynomial for the background gives the following results:

$$\begin{array}{llrl} J/\psi \text{ mass:} & M & = 3119 \pm 8 & \text{MeV}/c^2 \\ J/\psi \text{ width:} & \Gamma(\text{obs}) & = 35 \pm 7 & \text{MeV}/c^2 \end{array}$$

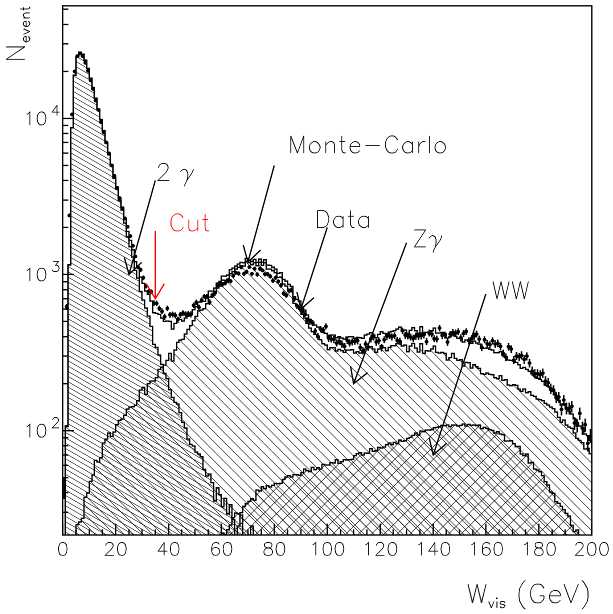

Figure 3: W_{vis} distributions for the data and for the simulated $\gamma\gamma \to$ hadrons, $e^+e^- \to Z^0\gamma$, $e^+e^- \to W^+W^-$ and the sum of all above Monte-Carlo contributions

The observed width of the peak is consistent within error with the invariant mass resolution of the pair of charged tracks in the mass region around $3\,\text{GeV}/c^2$. The number of observed events is $N(J/\psi) = 36 \pm 7$ from the fit. If we take the L3 result[7] on beauty cross section from $\gamma\gamma$ events and the PDG value[8] for the branching ratio of beauty hadrons to J/ψ, the expected number of $J/\psi \to \mu^+\mu^-$ from beauty hadrons is 2.1 ± 0.6. The backgrounds from the processes $\gamma + \gamma \to Z + \gamma \to J/\psi + X$ and $\gamma + \gamma \to \chi_{c2} \to J/\psi + \pi^+ + \pi^- + \pi^0$ are less than 0.20 and 0.30, respectively. According to selection criteria system X contains at least two charged tracks, hence we do not consider such sources of J/ψproduction as $\gamma + \gamma \to \chi_{c2} \to J/\psi + \gamma$.

For efficiency estimation we used the PYTHIA 6156 generator [9]. The generated events were passed through the simulation package of the DELPHI detector [10] and then processed with the same reconstruction and analysis programs as the real data. There is a substantial fraction of PYTHIA events where J/ψ's are produced just as a simple fusion of two photons because there is not enough phase space to produce additional particles. We checked that all such events are produced when both the colliding photons are direct or one photon is anomalous and the other one is DIS (we use here the PYTHIA notation, for the details see [9]). That is why for the efficiency estimation we did not use the events with direct-direct or DIS-anomalous photons. Among the rest of the PYTHIA events

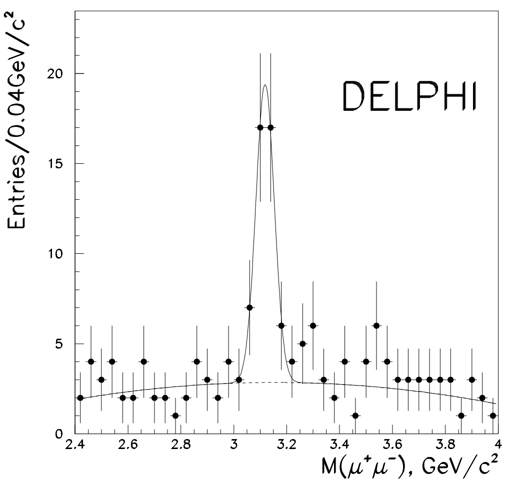

Figure 4: $M(\mu^+\mu^-)$ distribution from the DELPHI data. The solid curve corresponds to a Gaussian fit over a polynomial backgraound.

about 93% of the J/ψ's are produced when at least one photon is a VDM photon.

Fig. 5 shows the $p_T^2(J/\psi)$ distribution. As expected, the PYTHIA prediction for the $p_T^2(J/\psi)$ distribution is sharply peaked near zero for the diffractive MC events (see Fig.1), while the 'resolved' MC events (see Fig.2) are very much spread out. We fitted the experimental $p_T^2(J/\psi)$ distribution as a function of the two categories of MC events

$$\frac{\mathrm{d}N}{\mathrm{d}p_T^2} = f \cdot \left.\frac{\mathrm{d}N}{\mathrm{d}p_T^2}\right|_{\mathrm{Diffractive}} + (1-f) \cdot \left.\frac{\mathrm{d}N}{\mathrm{d}p_T^2}\right|_{\mathrm{Resolved}} \tag{5}$$

which gives $f = (26.0 \pm 22.0)\%$. The PYTHIA study tells us that the experimental efficiencies are very different for the two categories:

$$\begin{aligned} \epsilon(\text{diffractive}) &= (0.94 \pm 0.04)\% \\ \epsilon(\text{resolved}) &= (3.87 \pm 0.09)\% \end{aligned} \tag{6}$$

According to PYTHIA, about one-half of all the $\gamma\gamma$ events with $\psi \to \mu^+\mu^-$ are produced with the charged tracks at polar angles below 10 degrees, so that they are 'invisible to the DELPHI detector. The individual efficiencies as a function of p_T^2 are given in Fig. 6. One gains some insight into these efficiencies, if they are broken down into products of two factors, as follows:

$$\begin{aligned} \epsilon(\text{diffractive}) &= \epsilon_{\gamma\gamma}(\text{diffractive}) \times \epsilon_{J/\psi\to\mu^+\mu^-}(\text{diffractive}) \\ \epsilon(\text{resolved}) &= \epsilon_{\gamma\gamma}(\text{resolved}) \times \epsilon_{J/\psi\to\mu^+\mu^-}(\text{resolved}) \end{aligned} \tag{7}$$

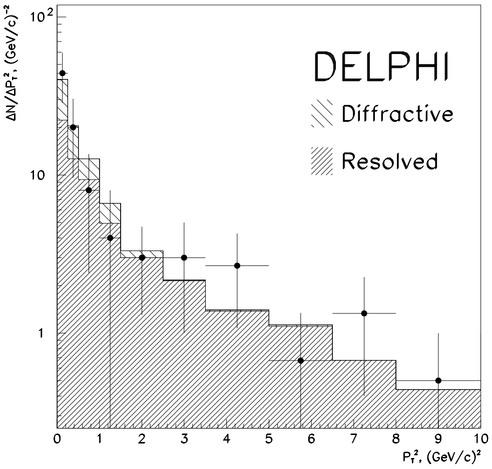

Figure 5: $p_T^2(J/\psi)$ distribution from the DELPHI data, shown as points with error bars. The histogram is a composite of the renormalized 'resolved' and 'diffractive' processes from PYTHIA (see text).

where $\epsilon_{\gamma\gamma}$ is the efficiency for the process $\gamma\gamma \to J/\psi + X$ and $\epsilon_{J/\psi\to\mu^+\mu^-}$ is that for $J/\psi \to \mu^+\mu^-$. As expected, the latter is relatively process-independent

$$\begin{aligned} \epsilon_{J/\psi\to\mu^+\mu^-}(\text{diffractive}) &= (37.0 \pm 1.5)\% \\ \epsilon_{J/\psi\to\mu^+\mu^-}(\text{resolved}) &= (32.1 \pm 0.7)\% \end{aligned} \tag{8}$$

It is clear, therefore, that the difference in efficiency in (6) is mostly due to $\epsilon_{\gamma\gamma}$—this is highly process-dependent and hence model-dependent.

The overall experimental efficiency is

$$\frac{1}{\epsilon} = \frac{f}{\epsilon(\text{diffractive})} + \frac{1-f}{\epsilon(\text{resolved})} \quad \begin{cases} 0 < f < 1 \\ \epsilon(\text{diffractive}) > 0,\ \epsilon(\text{resolved}) > 0 \end{cases} \tag{9}$$

which gives $\epsilon = (3.93 \begin{array}{c} + 2.18 \\ - 1.03 \end{array})\%$. Under the assumption that PYTHIA captures the kinematical features of the resolved and diffractive processes—but not their absolute cross sections—the cross section for inclusive J/ψ production is

$$\sigma = N(\psi) \cdot (Br \cdot \mathcal{L} \cdot \epsilon)^{-1} = 45.3 \pm 18.4 \text{ pb} \tag{10}$$

where $Br = (5.88 \pm 0.10)\%$ is the branching ratio for $J/\psi \to \mu^+\mu^-$ [8] and $\mathcal{L} = 617\,\text{pb}^{-1}$ is the total integrated luminosity. The quoted error reflects only that associated with the visible part of the spectra; in particular, it does not include the uncertainties inherent in the PYTHIA program. Because of the model-dependent aspect of this analysis (see, for example, the efficiencies given in (6)), it may be of interest to quote the 'visible' cross section. Substituting $\epsilon_{J/\psi\to\mu^+\mu^-}(\text{diffractive})$ and $\epsilon_{J/\psi\to\mu^+\mu^-}(\text{resolved})$ for $\epsilon(\text{diffractive})$ and $\epsilon(\text{resolved})$—respectively—in (9), the 'visible' cross section can be calculated; it is

$$\sigma_{\text{vis}} = 2.98 \pm 0.58 \text{ pb} \tag{11}$$

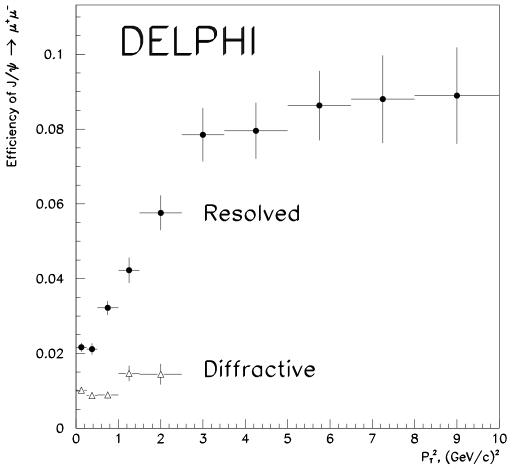

Figure 6: Efficiencies for resolved and diffractive processes as functions of p_T^2.

Following the same line of philosophy, we also give the 'visible' production rate $\langle n \rangle$ for J/ψ production

$$\langle n \rangle = N(\psi) \cdot \left(N_t \cdot Br \cdot \epsilon_{J/\psi \to \mu^+\mu^-} \right)^{-1} = (6.7 \pm 1.3) \times 10^{-3} \tag{12}$$

where N_t is the data sample for the $\gamma\gamma$ selection as given in the previous section, i.e. $N_t = 274\,510$.

The rapidity distribution for the J/ψ is shown in Fig. 7. The PYTHIA MC events have been combined using the same fraction f found in (5) and then normalized to the observed number of events in $0 < |y| < 2.0$. It is seen that the MC events are in fair agreement with the experimental rapidity distribution, although the data tend to have some deficiency below $|y| = 0.4$ (but not statistically significant). The same techniques have been used to compare the experimental distributions of $M(X_{\rm vis})$, $M(J/\psi + X_{\rm vis})$, the total and charged multiplicities [$N_{\rm tot}(X_{\rm vis})$ and $N_{\rm ch}(X_{\rm vis})$], in Figs. 8, 9, 10 and 11. There is fair agreement between the shape of our measured distributions and the PYTHIA predictions (using the best fit for the relative content of diffractive and resolved events and renormalizing the PYTHIA prediction to the number of observed events).

In figs.12 (a–c) are shown the acceptance-corrected distributions in $\cos\theta$ where θ is the helicity angle of μ^+ in the rest frame of $\psi \to \mu^+\mu^-$, along with the results of a fit to the form $1 + a\,\cos^2\theta$. The fitted parameters are $a = -0.93 \pm 0.57$ for the total sample (a), $a = -1.76 \pm 0.53$ for $p_T^2(J/\psi) < 1.0$ GeV/c (b) and $a = 0.71 \pm 1.33$ for $p_T^2(J/\psi) > 1.0$ GeV/c (c). These results demonstrate that the J/ψ's are produced with little polarization at high $p_T^2(J/\psi)$, where the main contribution comes from the resolved processes.

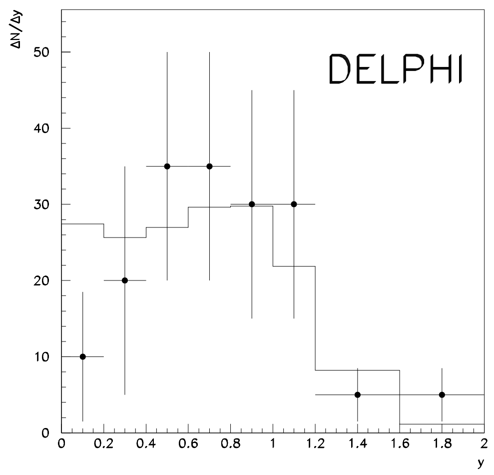

Figure 7: $|y|$ distribution for the J/ψ from the DELPHI data, shown as points with error bars. The histogram is a composite of the renormalized 'resolved' and 'diffractive' processes from PYTHIA (see text).

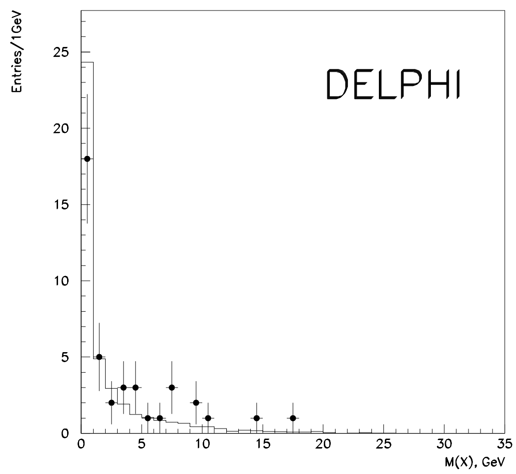

Figure 8: $M(X_{\mathrm{vis}})$distribution for the $J/\psi + X_{\mathrm{vis}}$ from the DELPHI data, shown as points with error bars. The histogram is a composite of the renormalized 'resolved' and 'diffractive' processes from PYTHIA (see text).

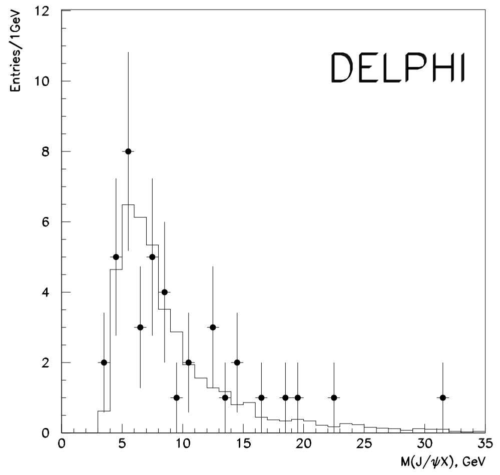

Figure 9: $M(J/\psi + X_{\text{vis}})$ distribution from the DELPHI data, shown as points with error bars. The histogram is a composite of the renormalized 'resolved' and 'diffractive' processes from PYTHIA (see text).

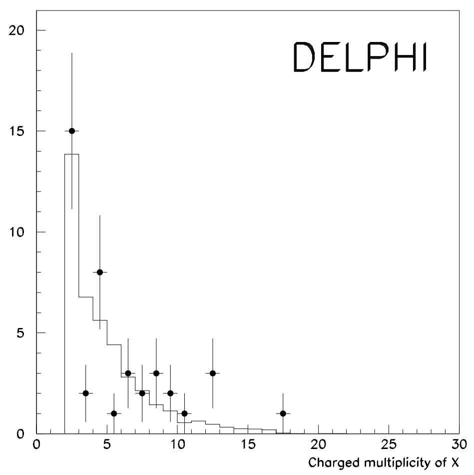

Figure 10: Total multiplicity $[N_{\text{tot}}(X_{\text{vis}})]$ distribution for the $J/\psi + X_{\text{vis}}$ from the DELPHI data, shown as points with error bars. The histogram is a composite of the renormalized 'resolved' and 'diffractive' processes from PYTHIA (see text).

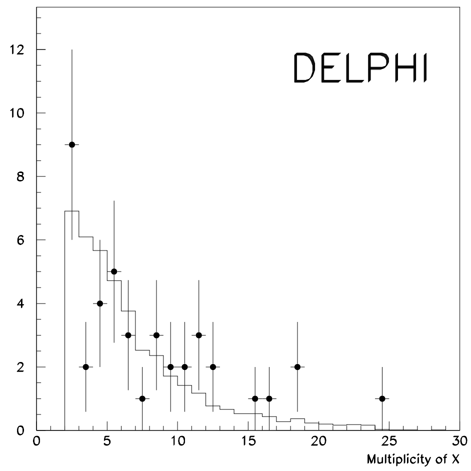

Figure 11: Charged multiplicity [$N_{\rm ch}(X_{\rm vis})$] distribution for the $J/\psi + X_{\rm vis}$ from the DELPHI data, shown as points with error bars. The histogram is a composite of the renormalized 'resolved' and 'diffractive' processes from PYTHIA (see text).

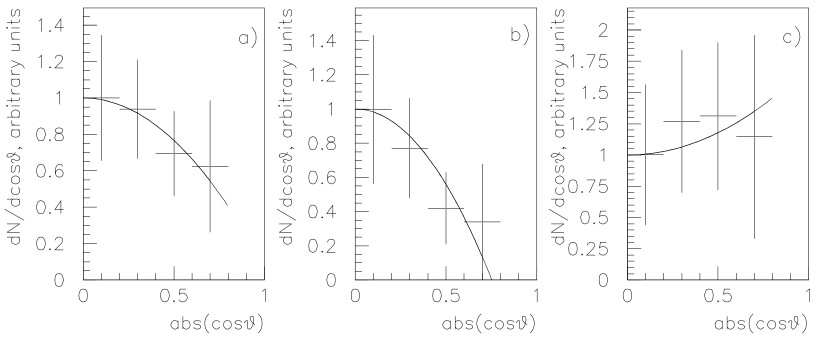

Figure 12: Acceptance-corrected distributions in $\cos\theta$ where θ is the helicity angle of μ^+ in the rest frame of $\psi \to \mu^+\mu^-$. The figures (a–c) correspond to the total sample (a), those with $p_T^2(J/\psi) < 1.0$ (GeV/c)^2 (b) and $p_T^2(J/\psi) > 1.0$ (GeV/c)^2 (c).

4 Conclusions

We have studied the inclusive J/ψ production from $\gamma\gamma$ collisions. The data have been taken by the DELPHI collaboration during the LEP II phase, i.e. $\sqrt{s}$ of the LEP machine ranged from 161 to 207 GeV. A clean signal from the reaction $\gamma\gamma \to J/\psi + X$ is seen.

The inclusive cross section is estimated to be $\sigma(J/\psi+X) = 45.3 \pm 18.4$ pb. Based on a study of the event shapes of different types of $\gamma\gamma$ processes in the PYTHIA program, we conclude that some $74 \pm 22\,\%$ of the observed J/ψ events are due to the 'resolved' photons, the dominant contribution of which is evidently derived from a single color-octet gluon within the photon [3].

The distributions in $p_T^2(J/\psi)$, y and $\cos\theta$ (for μ^+ in the rest frame of $J/\psi \to \mu^+\mu^-$) are presented. In addition, a study is given of the characteristics of the visible X and its multiplicities.

It is clear that theoretical models are still in the state of flux for the inclusive production of J/ψ's in two-photon fusion processes. Thus we anticipate an extended period of close collaboration between experimentalists and theorists, before emergence of a clear understanding of the nature of the processes involved and—with it—a more reliable estimate of the cross sections. We have made the first attempt at extracting the relative importance of the processes involved by fitting the observed $p_T^2(J/\psi)$ distribution as a supperposition of the same distributions from diffractive and resolved processes predicted by PYTHIA. We look forward to a further refinement of our analysis both with a future version of PYTHIA and other programs on the same topic.

Acknowledgements

We are indebted to Dr. T. Sjöstrand for his help with the diagrams included in this paper and for his comments on PYTHIA. We thank M. Klasen for his help with the diagrams important for inclusive J/ψ production. S.-U. Chung is grateful for the warm hospitality extended to him by the CERN staff during his sabbatical year in the EP Division.

References

[1] 'Physics ar LEP2,' edited by G. Altarelli, T. Sjöstrand and F. Zwirner, CERN96-01 (Vol. 1), Feb 1996.
See Section 7 (heavy-quark physics), p. 330, in the chapter on $\gamma\gamma$ physics.

[2] J.J. Sakurai and D. Schildknecht, Phys. Lett. **B40** (1979) 121;
I. F. Ginzburg and V.G. Serbo, Phys. Lett. **B109** (1982) 231.

[3] M. Klasen *et al.*, DESY 01-039 (April 2001);
R. M. Godbole *et al.*, LC-TH-2001-019 (February 2001);
E. L. Berger and D. Jones, Phys. Rev. D**23** (1981) 1521;
H. Jung, G. A. Schuler and J. Terrón, Int. J. Mod. Phys. A**7** (1992) 7955
B. Naroska, Nucl. Phys. B (Proc. Suppl.) **82** (2000) 187.

[4] P. Aarnio *et al.*, DELPHI Collab., Nucl. Inst. Meth. **A303** (1991) 233.

[5] P. Abreu *et al.*, DELPHI Collab., Nucl. Inst. Meth. **A378** (1996) 57.

[6] J. Ridky, V. Vrba, J. Chudoba, “ECTANA. User's Guide,” DELPHI/99-181 TRACK 96 (17 November 1999).

[7] R. R. McNeil *et al.*, Nucl. Phys. B (Proc. Suppl.) **82** (2000) 193.

[8] Review of Particle Physics, Eur. Phys. J. C**15**, (2000) 1.

[9] T. Sjöstrand, Comput. Phys. Comm. **82** (1994) 74.

[10] P.Aarnio *et al.*, DELPHI Collab., Nucl. Instr. Meth. A 378 (1996) 57.